

termine the conditions appropriate for the necessary uptake of nutrients by plants. Various factors such as soil bulk density, soil moisture content, pH and CaCO_3 content have been found to affect the diffusion of metallic ions in soils¹⁻⁴.

Rowell *et al*⁵ studied self-diffusion of sodium in soil and found an increase in the diffusion coefficient of ^{22}Na with an increase in moisture content. Recently Staunton and Nye⁶ reported that the ^{22}Na diffusion was independent of moisture content and bulk density. The present study was conducted to test the effect of soil bulk density and moisture content on ^{22}Na self-diffusion in silt loam soil of pH 8.5.

The diffusion coefficient (D) was measured by the method of Rowell *et al*⁵ using the following equation of Schofield and Graham-Bryce⁷ for the analysis:

$$Q_t/Q_\infty = \frac{1}{2}L(D.t/\pi)^{1/2}$$

where Q_t is the amount of ions which had diffused from active to non-active soil of the two half cells Q_∞ is one half of the total ^{22}Na in soil system, L is the length of cell in cm and t is the diffusion time (sec).

The results presented in table 1 indicate significant relationship between soil bulk density and moisture content. At 10% moisture level, as the bulk density increased from 1.25 to 1.6 g/cm³, due to compaction the pores were probably filled giving continuous liquid phase by bringing water films into close contact. On further increasing bulk density to 1.75 g/cm³ the soil particles were pushed much closer together. Hence the diffusing ions were forced to move around the particles which increased the tortuousness of diffusion path, resulting in the decrease in diffusion coefficient at 1.75 g/cm³. The ^{22}Na ion-soil particle interaction was minimum at soil bulk density of 1.6 g/cm³.

Further, the value of ^{22}Na self-diffusion coefficient increased with increase in the moisture from 10% to 20% (table 1). When moisture increases, the thickness of water films around soil particles increases reducing

the chemical interaction of ^{22}Na ions with soil particles. Due to higher moisture content, the continuity of liquid phase increases resulting in increased diffusion coefficient.

3 July 1984; Revised 11 October 1984

1. Phillips, R. E. and Brown, D. A., *Soil Sci. Soc. Am. Proc.*, 1965, **29**, 657.
2. Warncke, D. D. and Barber, S. A., *Soil Sci. Soc. Am. Proc.*, 1972, **36**, 42.
3. Hira, G. S. and Singh, N. T., *Soil Sci. Soc. Am. Proc.*, 1977, **41**, 537.
4. Singh, S. P., Sinha, M. K. and Randhawa, N. S., *J. Indian Soc. Soil Sci.*, 1983, **31**, 115.
5. Rowell, D. L., Martin, M. W. and Nye, P. H., *J. Soil Sci.*, 1967, **18**, 204.
6. Staunton, S. and Nye, P. H., *J. Soil Sci.*, 1983, **34**, 263.
7. Schofield, R. K. and Graham-Bryce, I. J., *Nature (London)*, 1960, **188**, 1048.

CATALYTIC DECOMPOSITION OF N_2O ON La_2MnMO_6 (M = Ni, Cu and Zn)

N. KAMESWARI, B. RAJASEKHAR,
R. RADHA and C. S. SWAMY

Department of Chemistry, Indian Institute of Technology,
Madras 600 036, India.

THE structure of a double perovskite allows stabilization of transition metal ions in their unusual oxidation states¹. This has stimulated considerable interest in identifying oxide systems crystallising in this structure to understand the relation between solid state properties and catalytic behaviour². The activity of $\text{La}_2\text{MnNiO}_6$ in the catalytic decomposition of 2-propanol has been reported earlier³. The catalytic activity of the compounds La_2MnMO_6 (M = Ni, Cu and Zn) towards the decomposition of N_2O is briefly discussed in this note.

The compounds have been synthesized by the solid state reaction between the component oxalate mixtures, by heating them in appropriate proportions in a Pt crucible, in air, at 960°C for 28 hr, with intermittent grindings. The compounds have been characterized by x-ray analysis, conductivity measurements using a two

Table 1 ^{22}Na self-diffusion coefficients.

Effect of bulk density at 10% moisture		Effect of moisture content at 1.75 g/cm ³ soil bulk density	
Soil bulk density (g/cm ³)	$D \times 10^7$ (cm ² /sec)	Moisture content (W/w)	$D \times 10^7$ (cm ² /sec)
1.25	3.4 ± 0.3	10%	17.8 ± 1.2
1.45	12.1 ± 0.9	15%	26.2 ± 1.9
1.60	19.7 ± 1.3	20%	38.1 ± 2.8
1.75	17.8 ± 1.2		

probe cell and magnetic measurements on a Guoy balance⁴. The decomposition has been carried-out on an all-glass static reactor provided with a recirculation assembly. The temperature range employed is 350–480 °C at initial pressures of 50 and 200 Torr of N₂O. The kinetic parameters have been evaluated using the corresponding no/strong inhibition rate equations, as shown below respectively.

$$-dP_{N_2O}/dt = k_1 P_{N_2O} \quad (1 - NI)$$

$$-dP_{N_2O}/dt = k_2 P_{N_2O}/(P_{O_2})^{1/2} \quad (2 - SI)$$

The results are reported in table 1 along with the solid state properties.

N₂O adsorption [corresponding to (1)] is found to be rate limiting on La₂MnNiO₆ at both the pressures whereas on La₂MnZnO₆, oxygen desorption⁴ is the slowest step. The compound La₂MnCuO₆ exhibited strong and no inhibition by oxygen at 200 and 50 Torr respectively, portraying the effect of pressure on the rate limiting step.

High magnetic moment on the catalyst (as in La₂MnNiO₆) facilitates the decoupling of the spins of the O²⁻ ion in the oxygen desorption step⁵, whereas the increases in *E_a* for conduction and lattice parameters along a series (table 1) decelerate the diffusion of O²⁻ ions on the surface. Based on these grounds, the applicability of different rate equations on these catalysts could be well understood.

Table 1 Physicochemical Properties of La₂MnMO₆

Property	Catalyst		
	La ₂ MnNiO ₆	La ₂ MnCuO ₆	La ₂ MnZnO ₆
Symmetry	Cubic	Cubic	Cubic
Cell Parameter, a (Å)	7.76	7.80	7.81
<i>E_a</i> for conduction (eV)	0.26	0.30	High resistivity
μ _{eff} (BM)	2.813	2.047	1.391
Sign of Seebeck Potential	+ve	+ve	–ve
Binding Energies (kcal/mole)	59.34	55.98	55.90
Rate Equation obeyed at 50 Torr	NI	NI	SI
Rate Equation obeyed at 200 Torr	NI	SI	SI
<i>E_a</i> for reaction at 50 Torr (kcal/mole)	16.3	4.2	5.3
<i>E_a</i> for reaction at 200 Torr (kcal/mole)	14.3	13.9	3.7
lnA for reaction at 50 Torr	4.6	–3.0	5.3
lnA for reaction at 200 Torr	2.6	4.2	3.7

At 50 Torr, the order of activities based on percentage conversions (table 1), for the three catalysts, in the temperature range 350–450 °C, is



In nitrous oxide decomposition reaction, *n*-type oxides are generally much less reactive than *P*-type oxides⁶. But in the present investigation, La₂MnZnO₆, even though it is an *n*-type oxide, exhibited highest percentage conversions at all temperatures. This may partly be due to the highly isolated Mn³⁺ ions present in the inert oxide matrix⁷, which are the result of slight non-stoichiometry of the compound.

When the present series of compounds is compared with the series La₂TiMO₆ (M = Ni, Cu and Zn) for N₂O decomposition at 200 Torr⁸ (table 2), the very low *E_a* for reaction and lnA values suggest a larger multipoint-mode of adsorption⁹ on the series La₂MnMO₆. One can visualize different types of clusters on mixed oxides of the type discussed here. Clusters of the type Mn–O–M are probably the active sites in the series La₂MnMO₆, owing to the availability of *d* electrons on the Mn ion. The lower lattice parameters for the Mn-substituted series also favour multipoint-adsorption. The lower M–O binding energies in the series La₂MnMO₆ as compared to La₂TiMO₆ may reduce the *E_a* for reaction to certain extent.

One of the authors (NK) acknowledges the Department of Atomic Energy, Government of India for the award of fellowship.

Table 2 Results of N₂O decomposition at 200 Torr on La₂TiMO₆

Compound	Rate Eqn. obeyed	<i>E_a</i> (kcal/mole)	lnA	Binding Energy (kcal/mole)
La ₂ TiNiO ₆	SI	3.6	–3.0	71.21
La ₂ TiCuO ₆	SI	21.5	10.1	67.89
La ₂ TiZnO ₆	SI	40.7	19.0	67.81

4 August 1984

1. Gilles Le Flem, Gerard Demazeau and Paul Hagenmuller, *J. Solid State Chem.*, 1982, **44**, 82.
2. Voorhoeve, R. J. H., *Science*, 1977, **195**, 827.
3. Radha, R. and Swamy, C. S., *Curr. Sci.*, 1983, **52**, 1012.

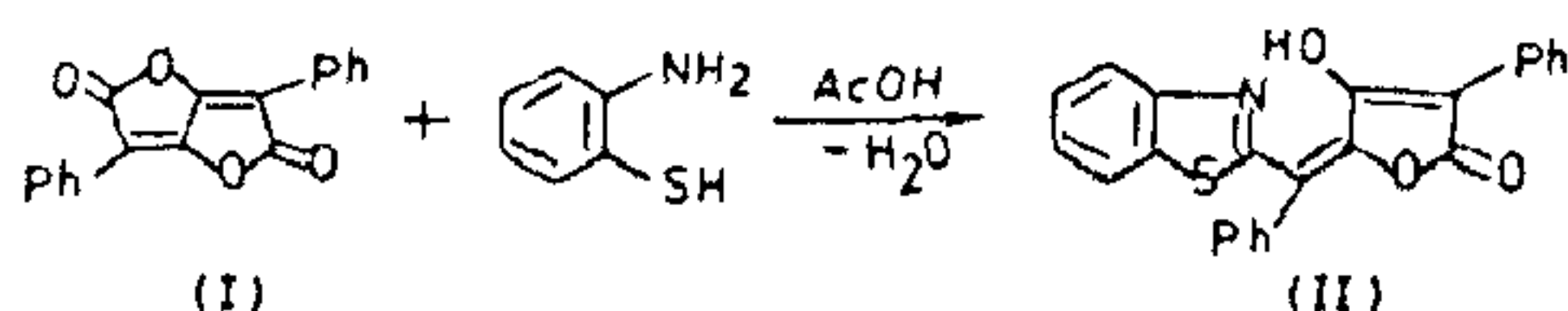
4. Ramanujachary, K. V., Kameswari, N. and Swamy, C. S., *J. Catal.*, 1984, **86**, 121.
5. Sastri, V. R., Pitchai, R. and Swamy, C. S., *Indian J. Chem.*, 1980, **19A**, 738.
6. Dell, R., Stone, F. S. and Tilley, P. F., *Far. Soc. Trans.*, 1982, **49**, 201.
7. Cimino, A. and Indovina, V., *J. Catal.*, 1970, **17**, 54.
8. Sastri, V. R., Pitchai, R. and Swamy, C. S., *Indian J. Chem.*, 1979, **18A**, 213.
9. Ramanujachary, K. V., Vijayakumar, K. V. and Swamy, C. S., *React. Kinet. Catal. Lett.*, 1982, **20**, 233.

CHEMISTRY OF LICHEN PRODUCTS— PART III: SYNTHESIS OF A NEW BENZOTHAZOLE DERIVATIVE FROM PULVINIC DILACTONE AND ITS PHYSIOLOGICAL ACTIVITY EVALUATION

K. RAGHAVA RAJU and P. S. RAO

Department of Chemistry, Kakatiya University,
Warangal 506 009, India.

PULVINIC dilactone¹, a lichen metabolite, possesses the tetronic acid ring system which is the essential feature of some biologically active natural products viz vitamin C and the cardenolide, digitoxigenin. Antibiotic activity of variabilin, strobilin and tetrenolin which contain 4-ylidene tetronic acid system is well known. 2-substituted benzothiazoles are shown to be active against dermatophytes, protozoans, gram-positive bacteria and even against the bacterial strains which are resistant to penicillin and viruses². Fungicidal activity of 2-amino derivatives is also well known³. With a view to synthesize new derivatives using lichen metabolites and to screen them for their antimicrobial activity, the present investigation was taken up. Pulvinic anhydride, which was prepared synthetically according to the procedure by Volhard⁴, was condensed with *o*-aminothiophenol in acid medium to yield the compound (II) (scheme 1). An excess of *o*-amino thiophenol did not alter the reaction from being equimolar suggesting the stability of the second lactone ring in the compound (I).



Scheme-I

The IR spectrum of the compound showed no absorptions either due to -SH group near 2850 cm^{-1} or amide carbonyl around $1620\text{--}1650\text{ cm}^{-1}$ region. It displayed a weak but broad absorption at 3400 cm^{-1} assignable to an enolic hydroxyl, a strong peak for lactonic carbonyl function at 1750 cm^{-1} and a peak at 1580 cm^{-1} due to C=N-stretching.

The PMR spectrum showed only two signals, one a cluster of complex multiplets in the region 7.4–8.5 ppm (14H) due to aromatic protons and a neat singlet at 13.6 ppm for enolic hydroxyl proton which was D_2O exchangeable.

High resolution mass spectrum of the compound confirmed the proposed structure. While the M^+ ion at m/z 397 corresponding to a formula $\text{C}_{24}\text{H}_{15}\text{O}_3\text{NS}$ was the second most intense peak, a signal at m/z 252 appeared to be the base peak. This M-145 fragment was formed by eliminating a neutral moiety which was characteristic of the compounds containing 4-ylidene tetronic acid skeleton. The other prominent peaks with sizeable intensity were at m/z 224 and 223 the first of which was formed from m/z 252 ion due to the loss of CO and the latter losing a hydrogen from the daughter ion. Other spectral fragmentations with their elemental analyses supported by the spectrum are shown in chart I.

Antibacterial Activity:

Antibacterial activity was studied *in vitro* using the cup plate method⁵. The bacteria employed were *Bacillus Polymixa*, *Bacillus pumilus* and *Streptococcus albus* (all gram positive) and *Proteus vulgaris*, *Pseudomonas ovalis* and *Acetobacter aerogenes* (all gram-negative). While the compound showed no activity against gram-positive bacteria it was moderately active against the gram-negative ones.

Antifungal activity:

The fungicidal activity⁶ of the compound (II) was assayed against two phytopathogenic fungi viz.

Drechslera rostrata and *Alternaria alternata* by spore germination method in acetone. The compound exhibited strong fungicidal activity against both the organisms inhibiting the growth completely at $200\text{ }\mu\text{g/ml}$ concentration. The log Ed_{50} values for *D. rostrata* and *A. alternata* were 2.2 and 2.08 respectively.

Melting point determined in an open capillary was uncorrected. Homogeneity of the compound was checked by TLC on plate coated (0.25 mm) with